Mechatronics 51 (2018) 115–126

Contents lists available at ScienceDirect

Mechatronics

journal homepage: www.elsevier.com/locate/mechatronics

The benefits of mechatronically-guided railway vehicles: A multi-body physics simulation study☆

Nabilah Farhat*, Christopher P. Ward, Roger M. Goodall, Roger Dixon

Wolfson School of Mechanical, Electrical and Manufacturing Engineering, Loughborough University, LE11 3TU, UK

ARTICLE INFO

Keywords:
Railway
Control
Active steering
Vehicle dynamics
Active guidance
Mechatronic vehicles

ABSTRACT

Mechatronically-guided railway vehicles are of paramount importance in addressing the increasing interest in reducing wheel-rail wear and improving guidance and steering. Conventional passively-guided rail vehicles are limited by the mechanical constraints of the suspension elements. Currently, a typical rail vehicle suspension needs to be sufficiently stiff to stabilize the wheelsets while being complaint enough to negotiate curved track profiles. The suspension is therefore a compromise for the contradictory requirements of curving and stability.

In mechatronic vehicles, actuators are used with the conventional suspension components to provide additional stiffness or damping forces needed to optimise a vehicle for a wide variety of scenarios, and not rely on a sub optimal combination of passive components.

This research demonstrates the benefits of active guidance and steering when compared to a conventional vehicle using simulation results from a multi-body simulation software Simpack. It also provides insights into the relative performance of the mechatronic schemes. The Simpack modeling allows for a complex model with high fidelity, which provides an additional level of proof of the control algorithms working on a real rail vehicle. Each vehicle is assessed in terms of guidance on straight track, steering on curved track, actuation requirements and wheel-rail wear. Significant benefits are demonstrated in one of the guided vehicles with independently-rotating wheelsets.

1. Introduction

This paper presents a comparison of a number of mechatronic steering concepts for rail vehicles with conventional bogies and draws comparisons on ride quality, actuation requirements, sensing requirements and track damage, using a conventional passively steered vehicle as a baseline. Ultimately, mechatronics promises a potential transformation of rail vehicles. However, the expectation is that implementations of such technology will be an incremental process and that the most straightforward modifications to a 'conventional' bogie will be a first step, with this paper considering the most applicable steering technology [1].

A typical rail vehicle consists of vehicle body, two bogies and four wheelsets as shown in Fig. 1. The conical tread of a conventional railway wheelset (two wheels solidly connected by an axle) provides a passive vehicle guidance mechanism that has been accepted best practice for nearly two centuries. However, this conical profile also causes an unconstrained solid-axle wheelset to be marginally stable and oscillate along the track in a sinusoidal motion known as 'hunting' [2]. To avoid this problem, the yaw motion of the wheelsets is constrained by a stiff suspension, stabilizing the wheelsets but interfering with the natural curving action of the wheelset. This is a well-known problem and suspensions have to be designed to meet the contradictory requirements of curving and stability at high speeds, with vehicles optimised for a particular operating regime.

In addition to the kinematic steering mechanism, creep forces are generated by the movement of the wheels with respect to the railhead due to 'pure' rolling rarely being achieved by the conical geometry of the wheels. At normal adhesion conditions, lateral creep forces are a function of the lateral wheel-rail displacement and the wheelset yaw angle with respect to the rail, also known as angle of attack. On a curved section of track the angle of attack has to be sufficient to generate enough lateral creep force to balance the centripetal forces [4]. However, conventional wheelsets produce large unnecessary creep forces, particularly in the longitudinal direction due to the stiffness of the yaw suspension. These large creep forces lead to excessive wear (of both the rail head and the wheel tread) and unwanted noise.

Although there have been a number of innovations in bogie design, many authors suggest that passive suspensions have reached an optimum performance which is determined principally by the spring

☆ This paper was recommended for publication by Associate Editor Wolfgang Kemmetmüller.

* Corresponding author.
E-mail address: n.farhat@lboro.ac.uk (N. Farhat).

https://doi.org/10.1016/j.mechatronics.2018.03.008
Received 13 October 2017; Received in revised form 29 January 2018; Accepted 15 March 2018
0957-4158/ © 2018 The Authors. Published by Elsevier Ltd. This is an open access article under the CC BY license (http://creativecommons.org/licenses/BY/4.0/).

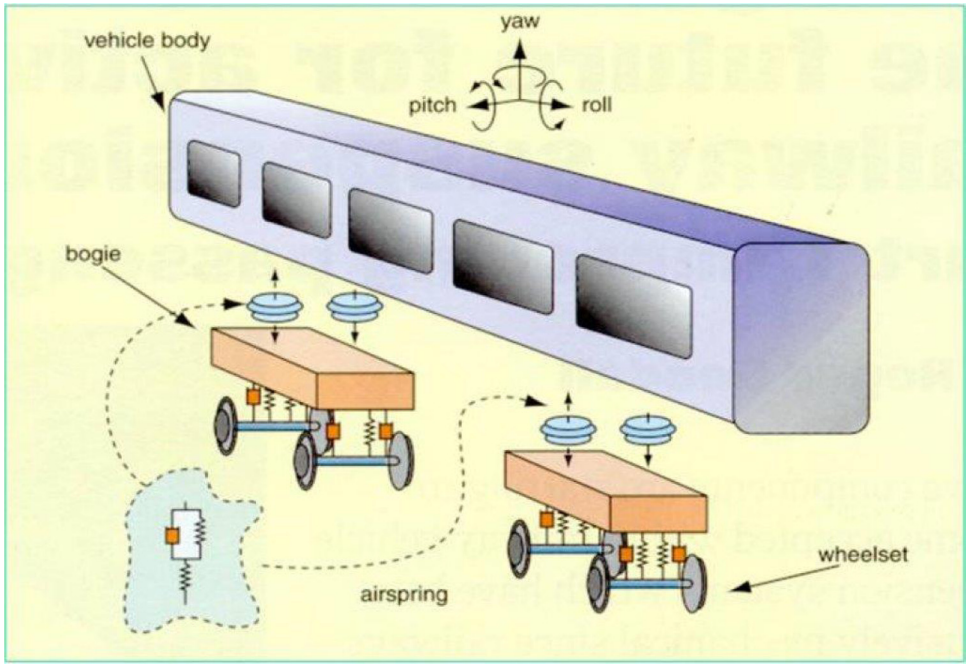

Fig. 1. Components of a railway vehicle [3].

stiffnesses, damper coefficients and their masses [5]. Active control has been suggested for some time now as an alternative way forward. The performance of an active suspension depends on sensors, actuators and the controller design in addition to the mechanical components. The wear due to traction, braking and balancing the centripetal forces is unavoidable, however the wear that is caused by the sub-optimal steering performance of the suspensions can be reduced dramatically by using active suspension concepts.

Active steering could be used to control the angle of attack to reduce the level of creep forces produced. Currently, the angle of attack of the wheels is maintained at acceptable values by bogies which shorten the distance between two wheelsets constrained in yaw. Active steering would make the functionality of bogies redundant, leading to the possibility of bogie-less vehicles which would be mechanically simpler [6]. Without a bogie, train floors could be lowered to create more internal space in the same loading gauge to accommodate double-deck trains in the UK. Active steering presents a range of possibilities from simply retrofitting actuators to current bogies through to completely redesigning vehicles to remove bogies. In this paper, the authors look at an incremental solution that balances the theoretical benefits of redesign with industrial reality. Normal adhesion conditions are considered at which the coefficient of friction has negligible effect on the guidance mechanism. Ideal sensing is assumed with a view that the performance benefits need to be established before the practicalities can be considered.

This paper considers three different active steering strategies that are applied to a full rail vehicle modeled using a multi-body simulation (MBS) software called Simpack. These are: Secondary Yaw Control (SYC), Actuated Solid-axle Wheelset (ASW) and Driven Independently-Rotating Wheelset (DIRW). Previous state-of-the-art papers have reviewed these active steering schemes and the control strategies associated with each [5,7]. The aim of this paper is to assess the performance of these active steering concepts in a non-linear simulation environment which takes into account complex vehicle dynamics and provides a far better representation of a real rail vehicle than previous simplified models. Note that the paper only considers steering and guidance and not traction and braking as the intention is to compare different active steering mechanisms under a broad set of track conditions. Section 2 explains the mechanical configuration of each of the steering concepts. Section 3 explains the vehicle modeling and track inputs used. The track inputs which the vehicle must follow are of two types - stochastic disturbances on a straight track which represent real track irregularities and a deterministic curve profile. The controller design process is explained in Section 4. Classical proportional integral (PI) and phase advance (PA) controllers are chosen for their simplicity and practicability. Finally, in Section 5 the performance of the different strategies is analysed in terms of the lateral/longitudinal creep forces, $T\gamma$ values which indicate wear levels and actuation requirements.

2. Active steering strategies

Control strategies for active steering are concerned with better guidance which eliminates all unnecessary creep forces and associated wheel-rail wear to achieve near-optimal performance of the running gear. In conventional rail vehicles, the front wheelset of the bogie produces large lateral creep forces while negotiating a curve. This poses a risk for derailment through flange climbing and the larger wheelset lateral force sets the limitation on the safe running speed of the vehicle. The lateral creep forces produced by the front and rear wheelsets should preferably be equal and sufficient to balance the centripetal forces. This is one of the conditions that must be satisfied for 'ideal' curving [4]. The second condition is that the longitudinal creep forces produced by the wheelsets should be zero, which is indicative of minimal wheel slip.

The active steering strategies discussed in this section involve both solid-axle and independently-rotating wheelsets (IRWs). IRWs produce negligible longitudinal creep forces as the wheels are able to roll at different speeds on the same axle to reduce slip. This is the reason why the power requirement of an IRW mechanism is lower than that of a solid-axle wheelset. The disadvantage is that IRWs require a guidance mechanism which needs to be provided by control action [8]. Traction and braking require that the left and right wheel longitudinal forces are balanced. The following is a description of three of the possible guidance methods that are applied to a bogie system. These are later compared to the passive vehicle model in Simpack described in Section 3.

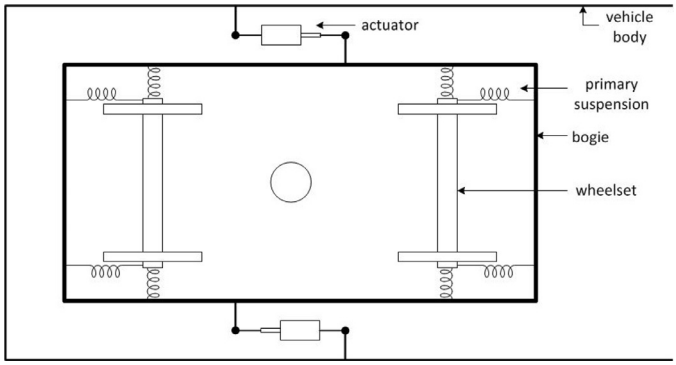

Fig. 2. Configuration for secondary yaw control.

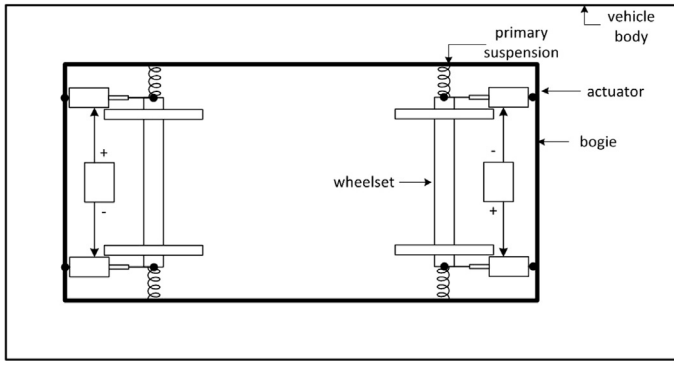

Fig. 3. Configuration for an actuated solid-axle wheelset.

2.1. Secondary yaw control (SYC)

In the secondary yaw control (SYC) scheme an actuator is placed between the bogie and the vehicle body in the same position as a traditional secondary yaw damper. The configuration is illustrated in Fig. 2. The control is therefore at the secondary suspension level instead of primary level because the idea is to balance the lateral creep forces on the two axles by applying a steering action to the bogie.

This configuration was studied by Braghin et al. [9] where on a straight track, the actuator force is proportional to the bogie/vehicle-body relative speed and opposite to it, much like a passive yaw damper. During curve negotiation, an additional force has to be provided which is obtained from a look-up table based on the curve radius, bogie yaw speed and vehicle speed. A limitation of this approach is that there are several look-up tables for different bogies, different friction coefficient values and wear levels, all of which are not easily accessible parameters in practice.

In a passive vehicle, if the primary yaw stiffness (PYS) is reduced, the curving performance improves but stability is compromised. SYC can also be used [10] to overcome the instability. The active control therefore does not improve curving, but allows the use of a soft PYS improving guidance whilst maintaining stability. A soft PYS has shown very significant decrease in wear and derailment coefficient, for the track conditions studied.

In this work, the primary longitudinal stiffness is reduced to 3.14 MN/m. The actuator provides the required yaw torque to the bogies which is determined using a PI (proportional plus integral) controller designed using classical frequency-domain design methods. The difference between the lateral creep forces at the wheel-rail contact of the front and rear wheelsets in each bogie is used as the feedback signal to calculate the control effort. This would therefore require estimation in practice using a model based filter, such as a Kalman–Bucy filter to estimate creep forces at the wheel-rail contact [11].

2.2. Actuated solid-axle wheelset (ASW)

An obvious strategy of implementing active steering is to apply a yaw torque directly to the wheelset. This can be done by either using a yaw actuator on each wheelset or a pair of longitudinal actuators working in opposition from the bogie to each axlebox to generate a yaw torque [12]. This configuration is illustrated in Fig. 3.

Curving performance can be improved by active yaw relaxation [10] where actuators are placed in series with longitudinal springs so that higher frequency oscillations of the wheelset are stabilised by the springs and low bandwidth active control is provided by the actuators. The yaw relaxation allows the wheelsets to take up their natural curving position. Simulation studies show that the leading wheelset has improved curving performance. In fact the trailing wheelset performance is worsened compared with the passive case, but this is to be expected because the lateral loads on the two wheelsets are now equalised, i.e. the trailing wheelset carries more lateral load during curving. For this work, the actuators are in parallel with the longitudinal springs to maintain a conventional suspension configuration. Typical longitudinal stiffness for a high speed train is in the 30–60 MN/m range [13]. The stiffness of the springs is reduced to 3.14 MN/m to lower the actuation torque required. The reduction in longitudinal stiffness allows the control mechanism to provide the stability without needing to overcome high stiffnesses. The control strategy uses the wheelset longitudinal creep force as the feedback signal and is illustrated in Fig. 4. The basic idea is to apply a yaw torque to the wheelsets to reduce the relative longitudinal forces between the contact points on the wheels and rails. This condition is referred to as ‘pure rolling’. Guidance is enhanced by the lower value of spring stiffness used. Similar to the previous configuration, an estimator will be needed to estimate the longitudinal creep forces which are used as feedback signals.

2.3. Driven independently rotating wheelset (DIRW)

Each wheel in the bogie is independently driven by its own drive-train as illustrated in Fig. 5. The basic concept is to maintain a difference in rotational speed of the wheels on curves and to drive the wheels on a straight track at the same speed (assuming there are no stochastic irregularities). The primary longitudinal stiffness is reduced to 3.14 MN/m to reduce the torque required. The feedback for guidance/steering is the relative speed of the wheels which is easily available because it is measured for traction/ braking purposes and can be used to implement a combined strategy for traction and steering [14]. Supplying traction separately to each wheel of a wheelset can produce a yaw torque which can be exploited to provide steering/ guidance control. The feedback for the traction control is usually the sum of the left and right wheel motor torques. This combined control can be used for enhancing fault tolerance which is a critical issue for actively steered vehicles. The mechanical integration of the wheel and the traction motor has been developed by SET Ltd. and a prototype “wheelmotor” was retrofitted to a Blackpool tram [15,16].

Controlling the speed of the motors creates an electronic axle and makes the wheelsets suffer from all the problems of a solid-axle wheelset including kinematic instability. Torque controlled motors however affect the rotational acceleration of the wheels, which causes them to have different angular positions and therefore not behave like solid-axle wheelsets [8]. In this study, the torque of the motors is controlled using a phase advance controller which uses the wheelset lateral displacement as feedback signal. Perfect sensing is assumed because the aim is to quantify the benefits for an ideal scenario. In reality, the wheelset lateral displacement is difficult to measure using inertial sensors on the wheelsets due to the high vibration environment. It can be measured using non-contacting sensors or estimated from bogie-mounted inertial sensors or a combination of both. However, estimators in the feedback loop can cause a drop in robustness of the

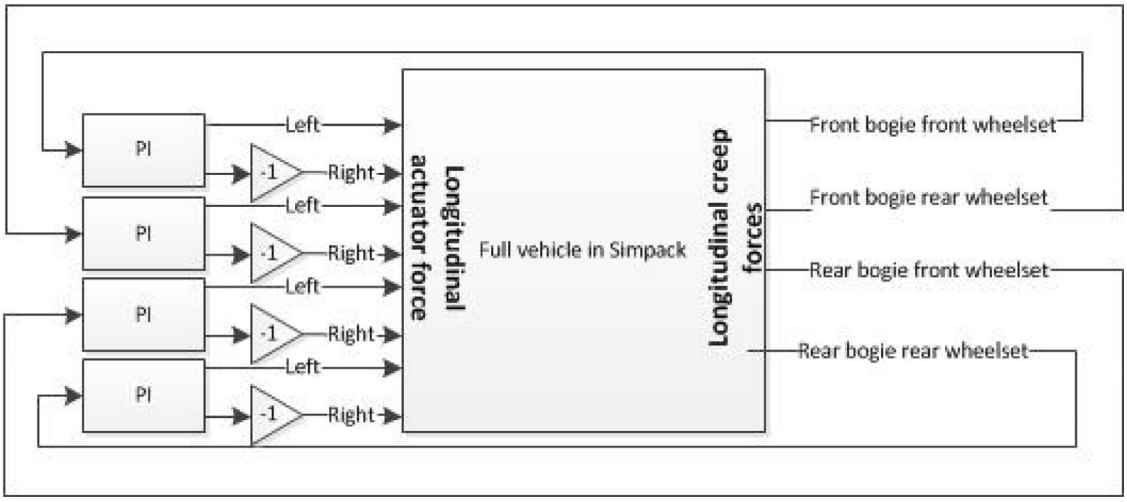

Fig. 4. Control of wheelset longitudinal creep forces.

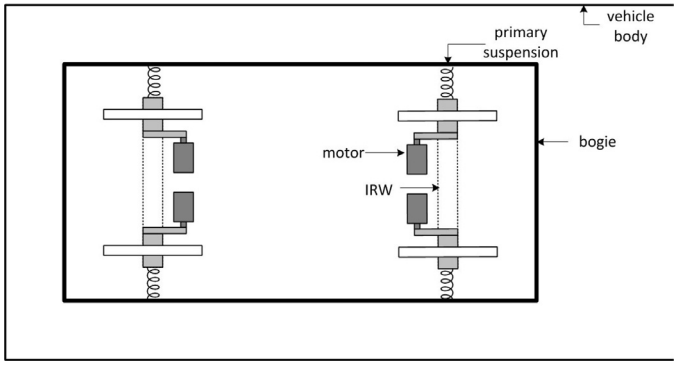

Fig. 5. Configuration for a driven independently rotating wheelset.

controller [12]. At present, New Measurement Trains used by Network Rail have laser-based systems to record measurements of track geometry for the purpose of rail maintenance [17].

3. Vehicle modeling

Two types of models sets were produced and are used throughout the paper. A non-linear Simpack vehicle model with the specific mechatronic actuation and sensing was developed for each of the three active vehicles and the passive benchmark. In addition, simplified linear 'design' models were used to perform frequency analysis and design the controllers. The linear models were developed using system identification methods where the input is a force or a torque to excite the system and the output is the resulting creep force or wheelset lateral displacement. System identification is chosen because it could be extended to a full scale vehicle when designing control algorithms, so is preferred for its ease of applicability. The correlation of the estimated system output and the Simpack model output is assessed by calculating the coefficient of determination or R^2 values. A value of 85% is set as the threshold above which the dominant dynamics of the Simpack model are captured to give an estimated model that is linear and behaves similarly to the Simpack model. The estimated linear 'design' models are used to perform frequency analysis to design controllers which are implemented on the nonlinear Simpack 'simulation' models. This design process is illustrated in Fig. 6. Once designed, the control algorithms in Simulink were applied on the Simpack model using co-simulation where MATLAB/Simulink ran in parallel with Simpack exchanging signals to close the control loop. Fig. 7 illustrates an overview of the complete co-simulation modeling environment. The 'simulation' models are a level up in complexity from the 'design' models and

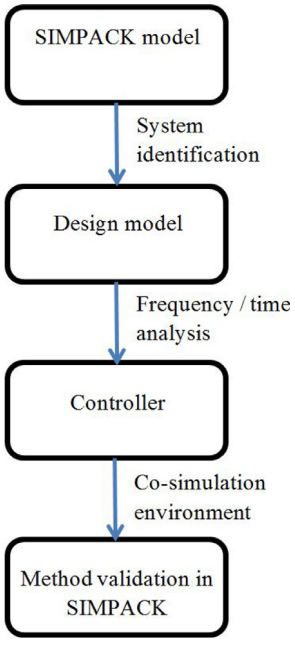

Fig. 6. Design methodology.

provide an additional level of proof that the algorithms will cope with parametric and structural uncertainty, as will be the case in application.

3.1. Simulation model

The Simpack model takes into account all of the vehicle degrees of freedom and allows movements between bodies that are considered to be effectively rigid. It accounts for the non-linearities in the rail-wheel profile and certain suspension components and this software is used by researchers and railway engineers in industry to model vehicle dynamics to an acceptable accuracy [18,19]. A review and comparison of the state-of-the-art of MBS software was undertaken as part of the "Manchester benchmark" project [20] indicating good correlation to reality. The interacting forces between bodies are defined through joint and force elements in Simpack so that the equations of motion don't have to be formulated directly by the user. The wheel-rail contact is modeled using the FASTSIM algorithm which is based on Kalker's "simplified theory", explained in detail in [21]. The contact is modeled by a series of three-spring systems such that each point within the contact patch between the wheel and rail can elastically displace in any

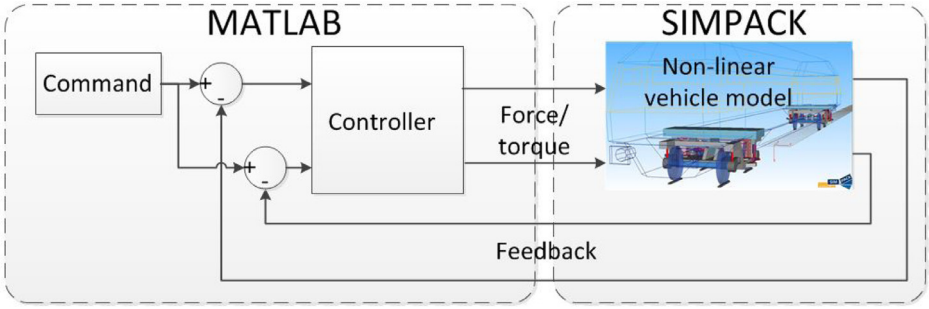

Fig. 7. Co-simulation overview.

Table 1
Parameter values used in the passive vehicle. In each of the active vehicles the primary longitudinal stiffness is reduced to 3.14 MN/m to reduce the actuation force/ torque required to overcome the suspension stiffness.

Symbol	Name	Value	Units
m_{bd}	Vehicle body mass	20,000	kg
m_b	Bogie mass	2615	kg
m	Wheelset mass	1200	kg
L	Half vehicle body length	11.2	m
a	Bogie semi-wheelbase	1.28	m
l	Half gauge width	0.75	m
c	Axlebox lateral semi-spacing	1	m
r_0	Wheel rolling radius	0.46	m
f_y	Primary lateral damper	6×10^5	Ns/m
k_y	Primary lateral spring	6.5×10^6	N/m
k_x	Primary longitudinal spring	3.14×10^7	N/m
f_{sy}	Secondary lateral damper	3×10^4	Ns/m
k_{sy}	Secondary lateral spring	1.6×10^5	N/m
$f_{s\psi}$	Secondary yaw damper	3.75×10^5	Ns/m
$k_{s\psi}$	Secondary yaw	5×10^6	N/m
R	Track radius of curvature	1200	m
θ_c	Track cant	4	deg
V	Vehicle speed	45	m/s

direction, independently of the neighboring contact points. FASTSIM provides a very good approximation and has a quick computation time which is why it is the accepted standard method [22]. The wheel and rail profiles selected are S1002 and UIC60 respectively with a rail inclination of 1:40. The mass and inertia of different bodies and the stiffness and damping of the suspension components in the model are chosen to represent a typical modern rail vehicle [23]. The main parameters are listed in Table 1.

3.2. Design model

All of the estimated models are ARX (autoregressive exogenous) models which have the following general form

$$A(z)y(k) = B(z)u(k-n) + e(k) \quad (1)$$

where u(k) is the system inputs, y(k) is the system outputs, e(k) is the system disturbance, n is the system delay, A(z) and B(z) are the polynomials as a function of the delay operator z^{-1}. The simulation is run on straight track with no stochastic disturbances and a small input torque is applied to excite the system dynamics. The input torque is a pulse with an amplitude of 10 kNm and a small width of 0.25 s to accentuate the higher frequencies to get a better estimated system. The amplitude is chosen to be high enough to excite the system while maintaining the wheel-rail contact non-linearities to a minimum.

For the SYC configuration, the input is a torque from the vehicle body to the front bogie. The output is the difference between the lateral creep forces of the front and rear wheelsets of the front bogie. The estimated system is a tenth order system and the estimated response has an R^2 metric of 94.14%. To apply system identification in the ASW configuration the input is a force applied from the bogie to the front wheelset. The output is the longitudinal creep force of the front wheelset. The estimated system is fourth order and the estimated response has an R^2 metric of 93.24%. Similarly for the DIRW configuration, the input is a motor torque applied to the right wheel of the front wheelset of the front bogie. The output is the lateral displacement of the front wheelset. The estimated system is fourth order and the estimated response has an R^2 metric of 86.15%. The results from the system identification of the three models are illustrated in Figs. 8–10 demonstrate the good correlation of the linear models to the non-linear dynamics, showing the applicability for controller design. This method could also be used to understand the dynamics of a full scale vehicle.

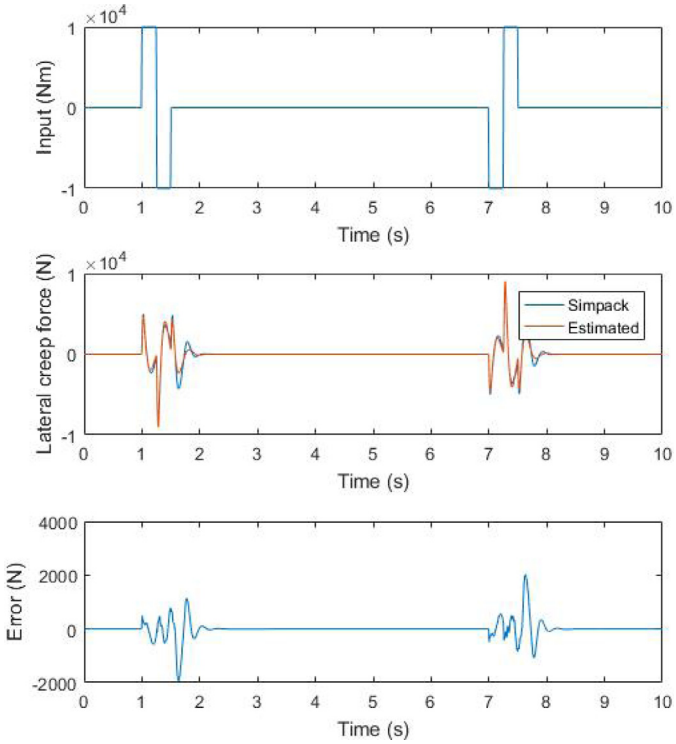

Fig. 8. System identification applied to the SYC model.

4. Controller design

In order to design the controller, the linear models are analysed in the frequency domain. For the frequency response a gain margin (GM) greater than 3 dB and a phase margin (PM) larger than 40° are commonly accepted to be good targets for a robust controller [24]. This is to accommodate for variations in plant dynamics or track disturbances. The gains for each of the controllers were chosen to meet the stability margins and give the desired time response with no steady state error.

For the SYC steering, a PI controller is chosen to remove any low frequency error signals. The feedback is the difference between the

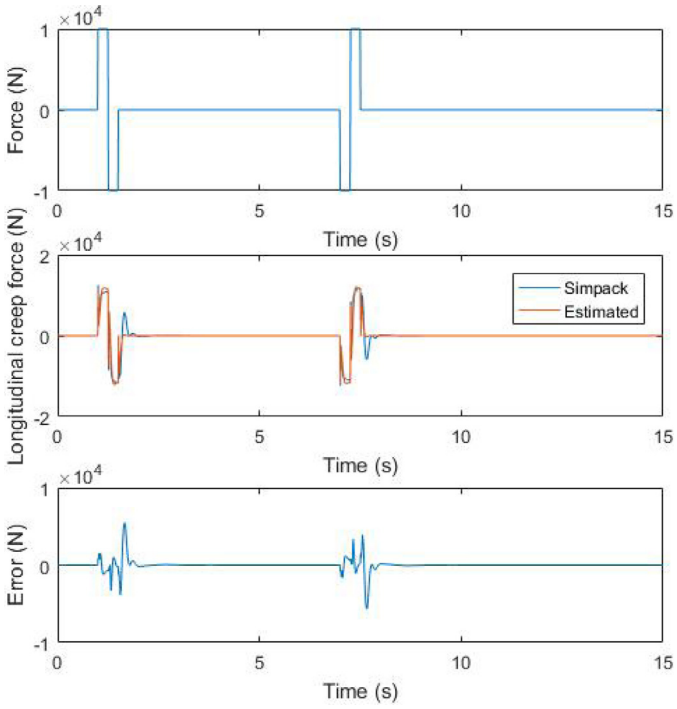

Fig. 9. System identification applied to the ASW model.

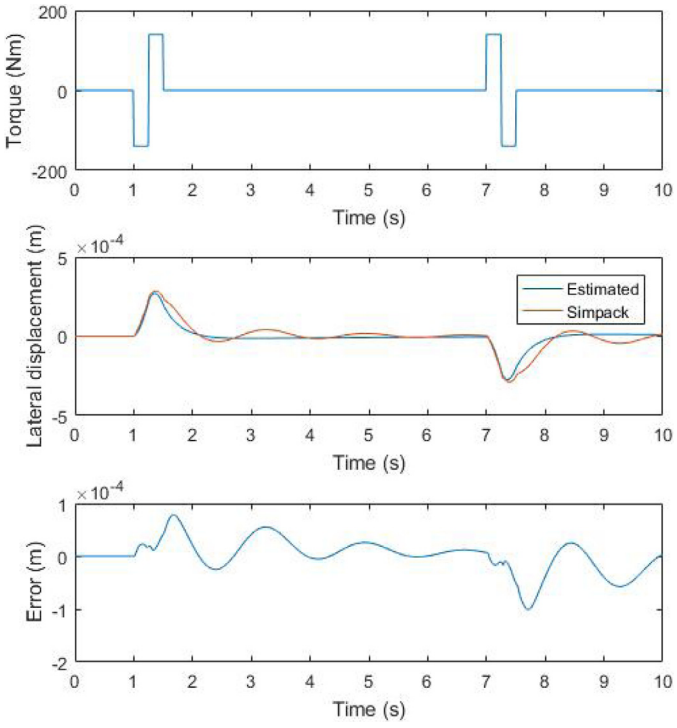

Fig. 10. System identification applied to the DIRW model.

lateral creep forces of the front and rear wheelsets in each bogie. The PI controller has the following transfer function

$$K(s) = \frac{K(1 + \tau s)}{\tau s} \tag{2}$$

A proportional gain K of 0.5 Nm/N and integrator time constant τ value of 0.01 s gives the desired frequency and time responses with no steady state error. Fig. 11 compares the open loop frequency response with and without the PI control applied in the SYC configuration. The controller

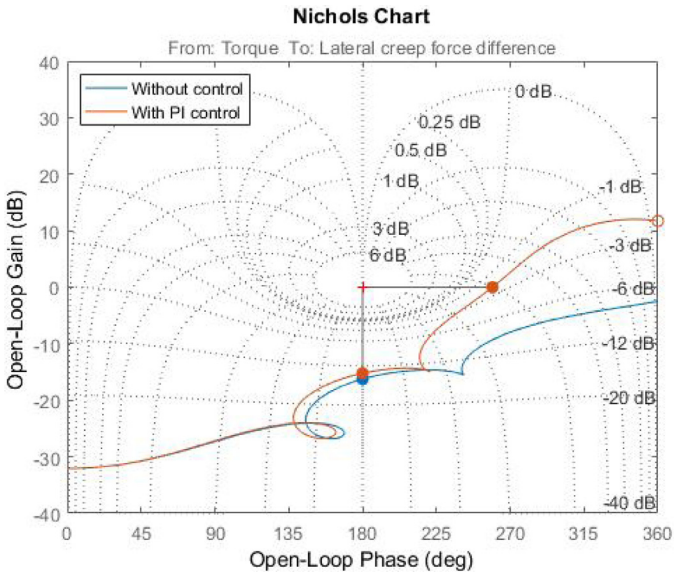

Fig. 11. Nichols plot for SYC controller design.

is given a zero demand signal, to equalise the lateral creep forces at the front and rear wheelsets of each bogie. As can be seen from the figure, the PI controller adds integral action at low frequencies to remove steady-state errors.

The controller for the ASW vehicle is also a PI controller with a K value of 0.7 N/N and a τ value of 0.1 s. Fig. 12 shows the open loop frequency reponse with and without the PI control in the ASW configuration. The longitudinal creep forces are used as the feedback signal. The aim is to reduce these to zero. For the DIRW configuration, a phase advance (PA) controller was chosen to overcome phase lag in the physical system and introduce more proportional gain without compromising stability. The feedback signal is the wheelset lateral displacement and the control effort aims to reduce this to zero. The controller used is in the form

$$K(s) = \frac{K_{pa}(1 + K_{ratio}\tau_l s)}{1 + \tau_l s} \tag{3}$$

where K_{pa}, K_{ratio} and τ_l values were selected to be 1.2×10^6 N/m, 6 and $2.5 \times 10^{-3}s$ respectively. Fig. 13 compares the open loop frequency

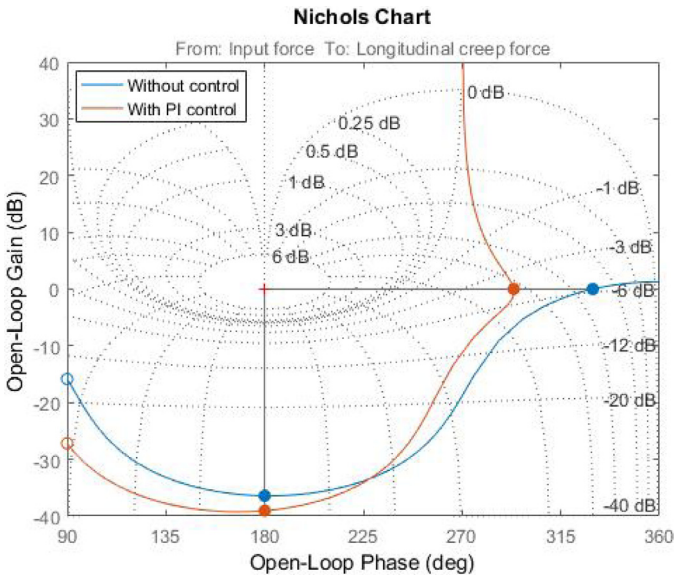

Fig. 12. Nichols plot for ASW controller design.

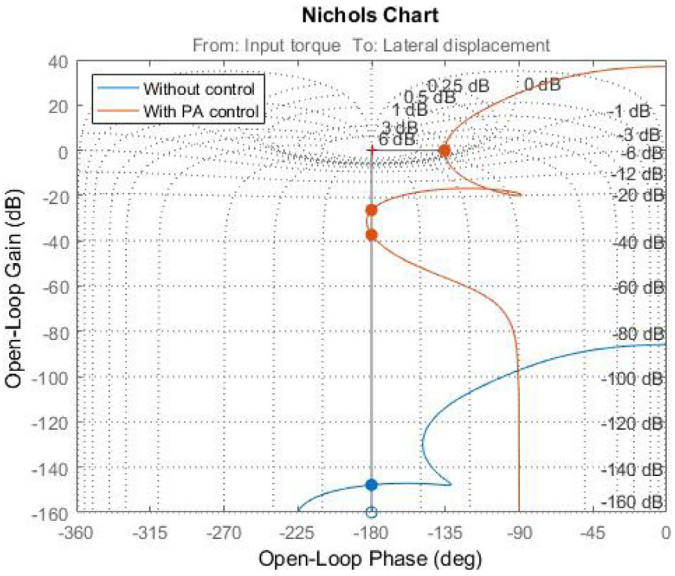

Fig. 13. Nichols plot for DIRW controller design.

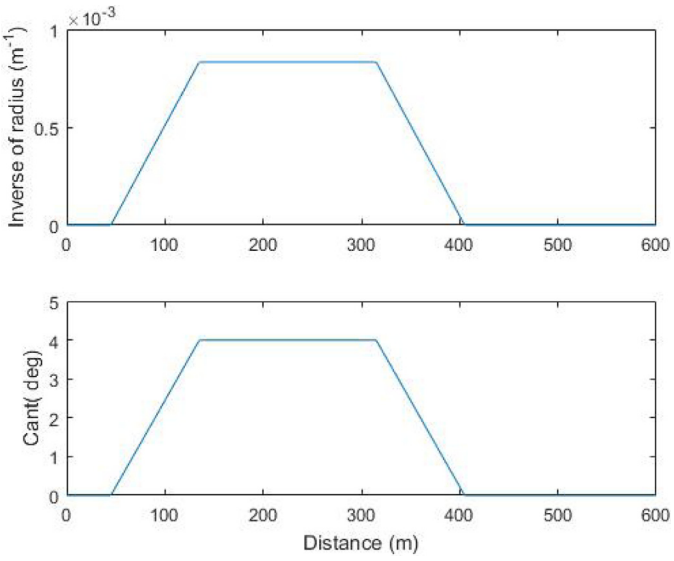

Fig. 14. Curved track radius and cant angle.

Table 2
System bandwidth and stability margins.

	GM (dB)	PM (deg)	Bandwidth (Hz)
SYC	15.2	79.1	6.2
ASW	39.1	114	1.07
DIRW	26.4	44.6	2.03

response with and without the PA control in the DIRW configuration. The PM of the DIRW configuration is relatively low compared to the other two models. Changing the controller gains to increase the PM worsens the creep force response of the model. Table 2 lists the stability margin and closed loop system bandwidth values for each of the active steering methodologies.

5. Performance analysis

5.1. Track profiles

For analysing the performance of all the actively steered vehicles a straight track with stochastic disturbances and three curved track profiles are used. One of the curved track profiles transitions linearly from a straight track at 40 m along the track to a curved track of radius 1200 m at 120 m. On a curve, the track is canted by an angle with respect to the horizontal plane. The track cant or superelevation also transitions accordingly with the curve transitioning back to a straight curve after 360 m. This is shown in Fig. 14. The required cant angle was calculated by using the equation

$$a = \frac{v^2}{R} - g\theta_c \tag{4}$$

where a is the lateral acceleration, R is the curve radius, v is the vehicle speed, g is acceleration due to gravity and θ_c is the cant angle. For the lateral acceleration experienced on the vehicle, known as the "cant deficiency" of 1 m/s^2, vehicle speed of 45 m/s and a curve with a radius of 1200 m, the cant angle is calculated to be 0.0698 rad or $\approx 4°$. 1 m/s^2 (10% g) cant deficiency is the accepted industry standard [25]. A similar calculation is also used to calculate the radius of curvature for a vehicle speed of 30 m/s with the same cant angle. This is the second track profile used.

The straight track profile is based on a recording car data from the Paddington to Bristol Great Western main line in the UK. It contains

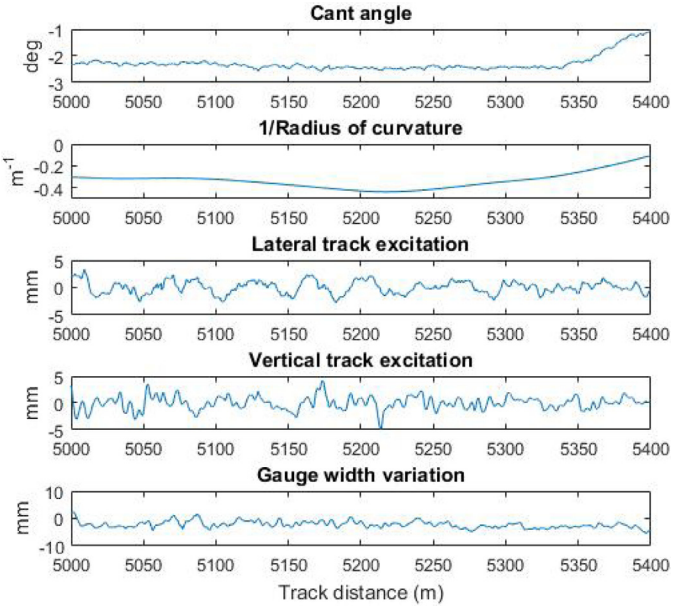

Fig. 15. Irregularities on the straight track profile.

track irregularities, sampled at 0.2 m, in the form of curvature and cant variation, lateral/ vertical excitation and gauge width variation as illustrated in Fig. 15. The higher speed curved track was also studied with the same lateral, vertical and gauge width stochastics as the straight track profile.

5.2. Performance indicators

The three active vehicles are compared against the passive solid-axle vehicle with no active control on the curved track and straight track scenarios. The following indicators are used to analyse the performance of each vehicle.

- *Lateral creep forces* of the front and rear wheelsets of each bogie should ideally be similar so that the safe running speed of a vehicle, which depends on the larger force of the front wheelset, can be increased.
- *Longitudinal creep forces* should ideally be zero to approach 'pure rolling' where the relative longitudinal speeds of the contact points

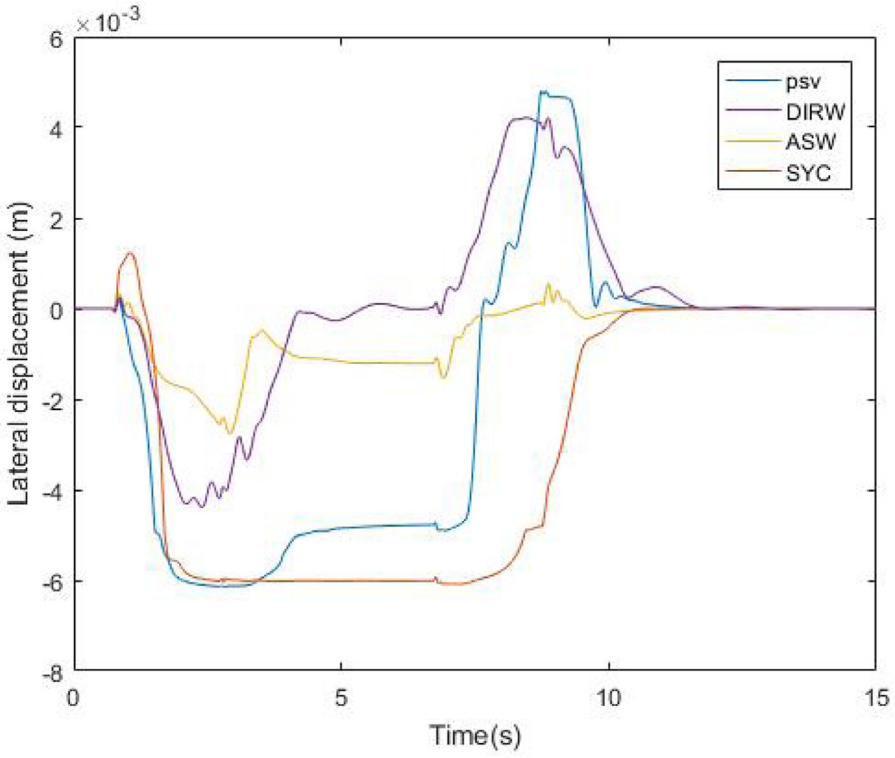

(a) Front bogie, front wheelset

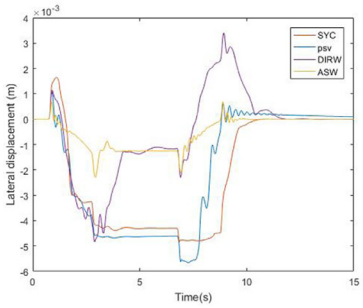

(b) Front bogie, rear wheelset

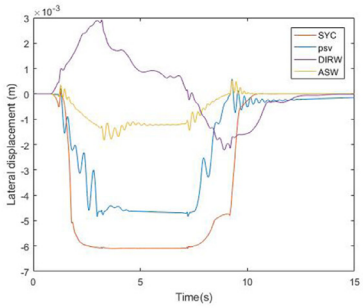

(c) Rear bogie, front wheelset

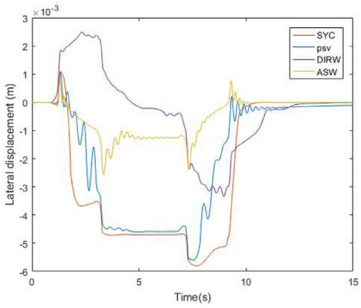

(d) Rear bogie, rear wheelset

Fig. 16. Lateral displacement of the wheelsets for all the mechanisms. The notations F_{WS}, R_{WS} and psv used in the graph labels mean 'front wheelset', 'rear wheelset' and 'passive' respectively.

on the wheel and rail are zero.

- *Wheelset lateral displacement* with respect to the rails should be less than 6 mm to minimise flange contact and resultant non-linearities.
- $T\gamma$, *Energy dissipated in the wheel-rail contact patch*, is used to give an indication of wear. It is calculated for each wheelset as

$$T\gamma = F_x\epsilon_x + F_y\epsilon_y \tag{5}$$

where F_x, F_y are the longitudinal and lateral creep forces and ϵ_x, ϵ_y are the longitudinal and lateral creepages respectively [26].

- *The actuation effort* must be achievable using an actuator physically small enough to fit in the desired space. Simple indicators such as maximum force and actuation power are used to ensure that the system is practically realisable with real actuators.

5.3. Creep forces and wheel-rail wear

Figs. 16–22 show the results from the simulation on the 1200 m radius curve without stochastics. Fig. 16 shows the lateral displacements of all the wheelsets for the 4 vehicles. The SYC vehicle hits the flange on the front wheelset of the front bogie and has a residual lateral displacement after the transition to straight track. This is contributing to the high undesirable longitudinal creep forces as shown in Fig. 17, which results in a higher $T\gamma$ value than that of the passive vehicle. The lateral creep forces illustrated in Fig. 18 look ideal and indicates that the controller is reducing the error between the feedback and the command to zero. However, the overall vehicle performance is worse than that of a passive vehicle due to flange contact, large residual longitudinal creep forces and high wear index. The control effort required is also therefore quite high peaking at about 60 kNm for each actuator between the vehicle body and the bogies. On the lower speed

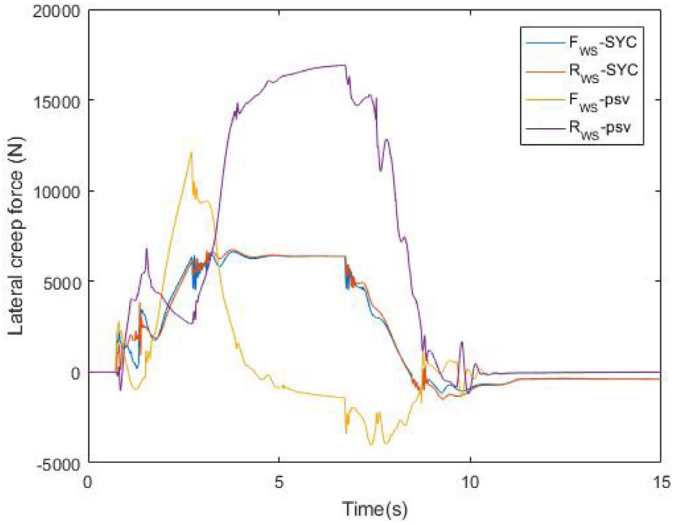

Fig. 17. Lateral creep force using SYC mechanism. The notations F_{WS}, R_{WS} and psv used in the graph labels mean 'front wheelset', 'rear wheelset' and 'passive' respectively.

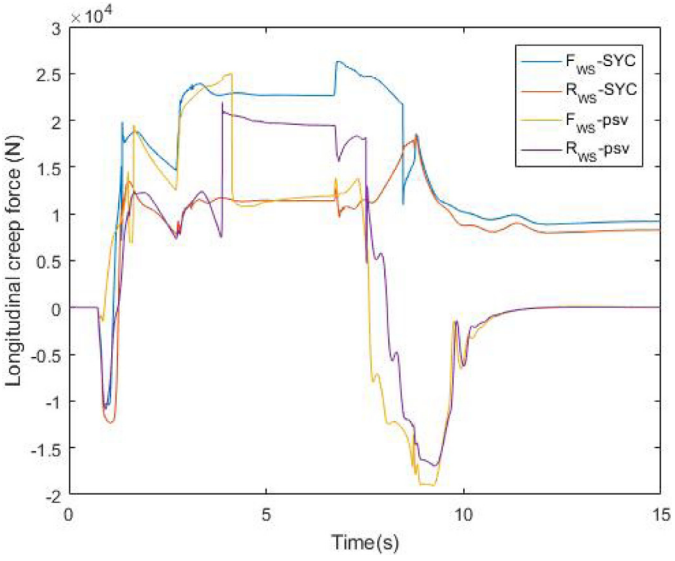

Fig. 18. Longitudinal creep force using SYC mechanism. The notations F_{WS}, R_{WS} and psv used in the graph labels mean 'front wheelset', 'rear wheelset' and 'passive' respectively.

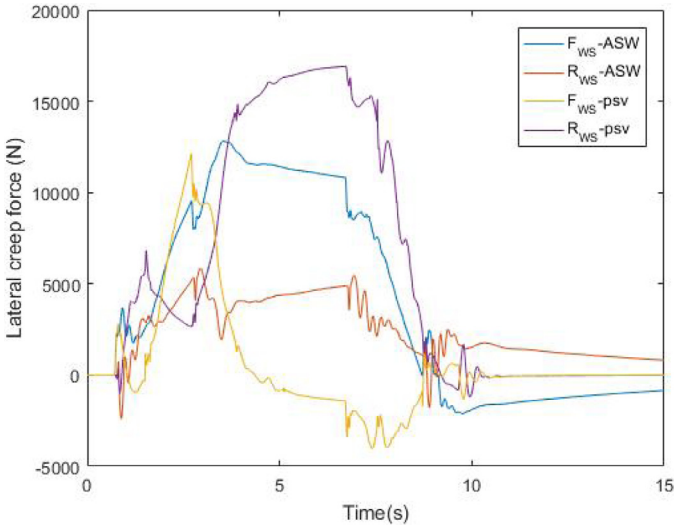

Fig. 19. Lateral creep force using ASW mechanism. The notations F_{WS}, R_{WS} and psv used in the graph labels mean 'front wheelset', 'rear wheelset' and 'passive' respectively.

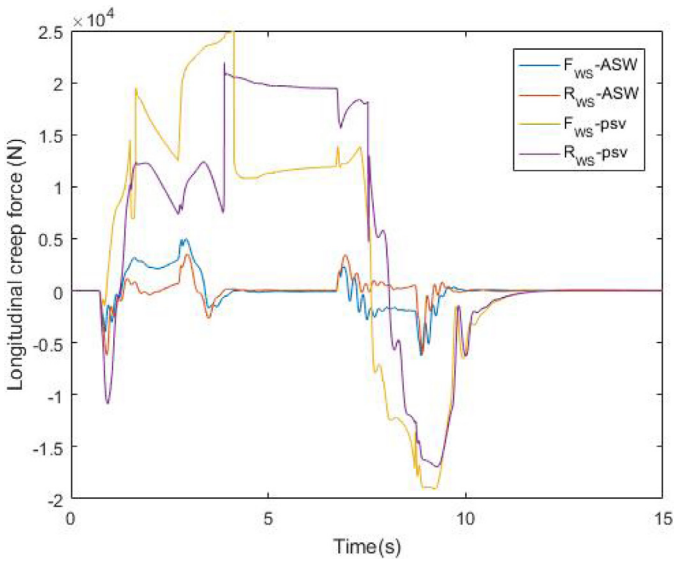

Fig. 20. Longitudinal creep force using ASW mechanism. The notations F_{WS}, R_{WS} and psv used in the graph labels mean 'front wheelset', 'rear wheelset' and 'passive' respectively.

curve, however, the SYC has an improvement in performance compared to the passive vehicle as indicated by a lower $T\gamma$ value in Table 3.

For the ASW vehicle the longitudinal creep forces shown in Fig. 20 are much lower than that of a passive vehicle. The difference in the lateral creep forces at the front and rear wheelsets is also reduced but is higher than that of a passive vehicle during transitions as shown in Fig. 19. The control torque is quite high with a peak of 40 kN for each longitudinal actuator. Theoretically the gain could be increased more because the gain margin is generous as indicated in Table 2, however doing so significantly increases the control effort required to levels that are not realisable in practice. The control torque can be reduced by placing the actuator in series with the longitudinal springs. The $T\gamma$ values in Table 3 indicate an overall reduction in wear in the ASW vehicle compared to the passive vehicle on all four track profiles considered.

The DIRW vehicle shows lower longitudinal creep forces than the passive vehicle in Fig. 22, however the wheels are not in pure rolling. Although the difference in the lateral creep forces of front and rear wheelsets is reduced as shown in Fig. 21, it is not eliminated completely. The DIRW concept relies on motor torques generating longitudinal creep forces to provide a yawing action to the wheelset. The longitudinal creep forces are lower than that of a conventional vehicle because only the forces necessary for steering are generated. Conventionally, large unnecessary longitudinal creep forces are generated due to the sub-optimal performance of the suspension. If the wheelset lateral displacement is not controlled to go to zero, the longitudinal creep forces can be reduced further and should contribute to a lower wear index value. This would also need lower actuation effort which peaks at about 6 kNm for each wheel motor. The low actuation requirement is due to the fact that the wheels are able to rotate independently of each other and therefore have very low slip. The DIRW vehicle has the lowest $T\gamma$ values compared to all the other vehicles as indicated in Tables 3 and 4.

5.4. Actuation requirements

The maximum force/ torque output from the actuators in each configuration is given in Table 5. The calculations are based on the straight track profile and the curved track with $R = 1200$ m without stochastics. Some examples of actuators that could be used in each

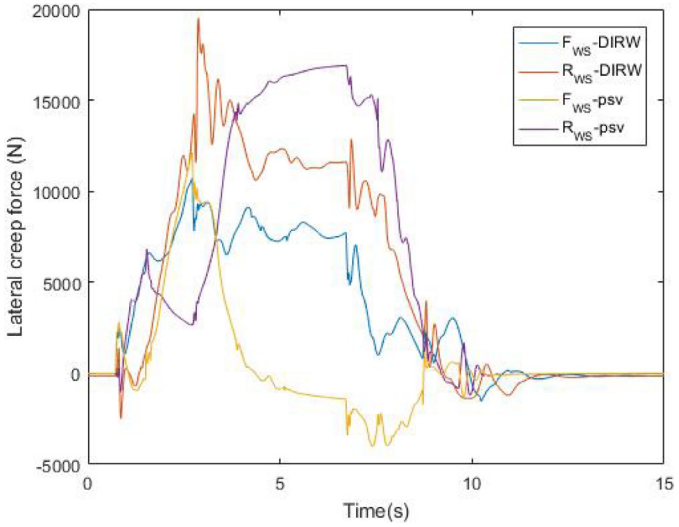

Fig. 21. Lateral creep force using DIRW mechanism. The notations F_{WS}, R_{WS} and psv used in the graph labels mean 'front wheelset', 'rear wheelset' and 'passive' respectively.

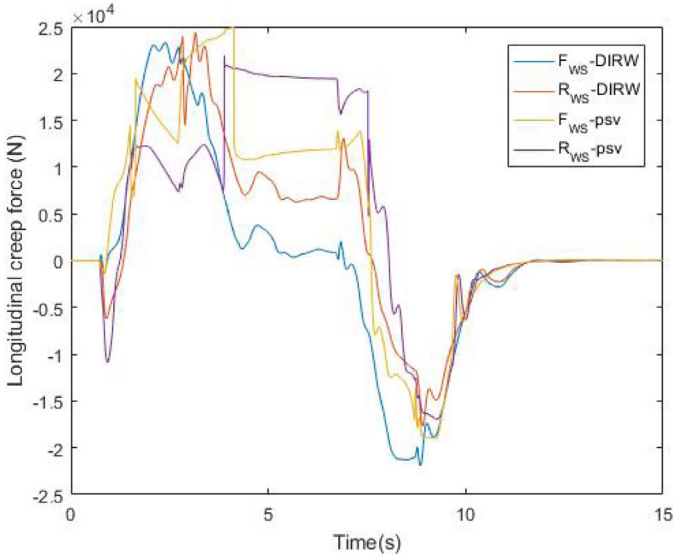

Fig. 22. Longitudinal creep force using DIRW mechanism. The notations F_{WS}, R_{WS} and psv used in the graph labels mean 'front wheelset', 'rear wheelset' and 'passive' respectively.

application are also listed which shows that the required control effort is achievable using readily available actuators of reasonable power consumption.

Power requirement is lowest for SYC vehicle on straight track due to the natural guidance mechanism of wheelsets as on a conventional vehicle. The DIRW mechanism power requirement is also much lower on straight track compared to the ASW mechanism as the control is not acting against the natural guidance of the wheelsets. In the curved track scenario, the transition period is fairly slow, leading to a low maximum velocity of the actuator for the SYC and ASW vehicles. The power consumption for the DIRW mechanism is still high because power is still required to drive one of the wheels faster and the other slower to follow the track centre line. The velocities of the two wheels on a single wheelset are not equal and opposite about the nominal velocity due to a net lateral displacement when the vehicle is negotiating a curve. This lateral displacement is necessary to provide the appropriate lateral creep forces. The power from the decelerating wheel is considered to be used to drive the accelerating wheel. It is important to note that although the maximum per wheel power consumption in the DIRW mechanism is 1.55 kW, this is only for a very short period during the transition from straight to curved track. On steady state it is approximately 200 W which is fractional compared to the power consumption of each wheel to drive the vehicle which is $\approx$ 100 kW.

Table 3
$T\gamma$ values on three different curved track profiles considered. Note that the cant for all the profiles is the same, $\approx 4^{\circ}$. Also note the units for the Tγ values is J/m.

Curved track at $R = 1200$ m, $v = 45$ m/s				
	Passive	SYC	ASW	DIRW
Front bogie front WS	30.03	21.55	9.92	0.15
Front bogie rear WS	10.25	0.64	1.77	0.08
Rear bogie front WS	1.72	59.92	1.22	1.49
Rear bogie rear WS	3.62	15.82	12.37	5.89
Total $T\gamma$ on all WSs	45.62	97.94	25.29	7.61
Percentage of passive	100	222.24	57.38	17.27
Curved track at $R = 534.52$ m, $v = 30$ m/s				
	Passive	SYC	ASW	DIRW
Front bogie front WS	84.47	16.85	15.44	1.13
Front bogie rear WS	4.99	2.10	0.24	0.84
Rear bogie front WS	26.16	48.94	1.56	10.23
Rear bogie rear WS	39.38	6.62	27.78	10.48
Total $T\gamma$ on all WSs	155.00	74.518	45.022	22.673
Percentage of passive	100	48.076	29.047	14.627
Curved track with stochastics at $R = 1200$ m, $v = 45$ m/s				
	Passive	SYC	ASW	DIRW
Front bogie front WS	13.59	22.42	10.45	1.39
Front bogie rear WS	12.31	1.19	2.18	0.63
Rear bogie front WS	0.57	59.42	1.23	2.20
Rear bogie rear WS	17.08	15.50	13.39	4.86
Total $T\gamma$ on all WSs	43.55	98.52	27.25	9.08
Percentage of passive	100	226.25	62.57	20.86

Table 4
$T\gamma$ values on straight track. Note the units for the Tγ values is J/m.

	Passive	SYC	ASW	DIRW
Front bogie front WS	0.81	15.22	3.89	1.21
Front bogie rear WS	18.99	13.52	3.04	2.89
Rear bogie front WS	0.34	24.19	2.05	7.70
Rear bogie rear WS	17.39	47.83	6.79	3.63
Total $T\gamma$ on all WSs	37.53	100.76	15.77	15.43
Percentage of passive	100	268.48	42.02	41.11

Inspite of the higher power requirement of the DIRW vehicle on a curved track, it appears to give the best solution. It shows the most significant improvement compared to a conventional vehicle in terms of reduced wear and minimal flange contact with much less actuation effort than the ASW mechanism which offers the next best performance.

Note:

1. Where there are two values separated by a '/', the first value indicates that for each actuator and the second is that per bogie. The force/ power values for each actuator for a particular mechanism are different and the 'per bogie' values are the sum of those on the front bogie.
2. For the curved track situation, average force and power values are not calculated as maximum values are more relevant when the rail vehicle is transitioning from straight to curved track and vice versa.
3. Maximum displacement for the DIRW mechanism is indicated as 'N/A'. The actuator displacement cannot be measured because the yawing of the wheelset is due to the relative torque of the two wheelmotors.

Table 5
Actuation requirements on straight and curved track with $R = 1200$ m.

Straight track requirements	SYC	ASW	DIRW
Average force/ torque	9.76/ 19.52 kN	9.6/ 22.93 kN	0.46/ 1.39 kNm
Maximum force/ torque	195/ 390 kN	79.4/ 518 kN	5.2/ 18.57 kNm
Average power	51.73/ 103.46 W	200/ 676.3 W	121/ 600 W
Maximum power	34/ 68 kW	69.4/ 169.3 kW	19/ 3.88 kW
Maximum displacement	5.37 mm	9.1 mm	N/A
Maximum velocity	1.54×10^{-1} m/s	2.05 m/s	104.4 rad/s
Curved track requirements	**SYC**	**ASW**	**DIRW**
Maximum force/ torque	16.39/ 32.78 kN	50.12/ 86.6 kN	5.37/ 21.76 kNm
Maximum power	79.22/ 158.44 W	198.59/ 448 W	1.55/ 2.31 kW
Maximum displacement	5 mm	3.6 mm	N/A
Maximum velocity	7.8×10^{-3} m/s	4.3×10^{-3} m/s	97.9 rad/s
Example actuator	MTS Series 244.31 [27]	Moog A085 [28]	Alstom 4 FXA 4553 [29]
Dimensions	Height = 664 mm Width = 216 mm	Height = 137.9 mm Width = 101.6 mm	Width × height × length = 890 × 890 × 942 mm

4. Maximum velocity for the DIRW mechanism can be misleading as it includes the nominal wheel rotational velocity which is 45/0.46 based on the vehicle running velocity and the nominal wheel radius.
5. The force and power requirements for the DIRW mechanism are calculated by isolating that required for the running of the vehicle to give a common platform to compare all three mechanisms.

6. Conclusions

This paper assesses three different control strategies using a non-linear vehicle model which is developed in an industry-standard software. Using an MBS simulation model provides a better representation of a real rail vehicle than previous simplified models.

From the active steering mechanisms studied in this work, the driven independently-rotating wheelsets show the best performance with a significant reduction in wear on straight and curved track. In the ASW and SYC vehicles the control action interferes with the natural behavior of a solid-axle wheelset which requires a higher actuation effort and is also detrimental to the wheel-rail wear. A more complex state-feedback controller could be used to 'trade-off' several desired characteristics and reduce the wheel-rail wear. However using a very simple controller on a non-linear vehicle model with high fidelity demonstrates the benefits of implementing active steering, especially on vehicles with IRWs. The DIRW vehicle requires the most radical change but promises the best performance.

Ideal sensing and actuation is assumed with the idea that further work is needed to consider the practical implementation of these active steering strategies. A further extension of this work could be to assess the sensing and actuation requirements of each of the schemes in more detail, taking into account actuator dynamics. Sensing the feedback signals is a challenge due to the high vibrations at the wheel-rail interface. A further extrapolation could also be done to conduct a similar study on bogie-less vehicles using the ASW and DIRW schemes. This of course requires a complete redesign of rail vehicles but has the potential to reduce their cost and mechanical complexity. The benefits of mechatronic vehicles are not only limited to the vehicle, but have the potential to reduce wear at switches and crossings. They could be fully controlled using on-board systems while running on a passive track.

Acknowledgments

The research has been supported by a Loughborough University studentship and European Unions Horizon 2020: the Framework Programme for Research and Innovation (2014–2020) through grant number 635900 for the project IN2RAIL: Innovative Intelligent Rail.

References

[1] Bombardier. Flexx tronic technology. 2008. http://www.bombardier.com/content/dam/Websites/bombardiercom/supporting-documents/BT/Bombardier-Transportation-ECO4-FLEXX_Tronic-EN.pdf [accessed 09-September-2016].
[2] Gilchrist AO. The long road to solution of the railway hunting and curving problems. Proc Inst Mech Eng 1998;212(3):219.
[3] Yusof HM. Technologies and control strategies for active railway suspension actuators, Ph.D. thesis. Loughborough University; 2013.
[4] Goodall R. Active suspension technology and its effect upon vehicle-track interaction. System dynamics and long-term behaviour of railway vehicles, track and subgrade. Springer Berlin Heidelberg; 2003. p. 35–50.
[5] Mei TX, Goodall RM. Recent development in active steering of railway vehicles. Veh Syst Dyn 2003;39(6):415–36.
[6] Ward CP, Mei TX, Hubbard P, Mirzapour M. Half cost trains: design for control. RRUKA. Loughborough University and University of Salford; 2013.
[7] Bruni S, Goodall R, Mei TX, Tsunashima H. Control and monitoring for railway vehicle dynamics. Veh Syst Dyn 2007;45(7–8):743–79.
[8] Mei TX, Goodall RM. Practical strategies for controlling railway wheelsets independently rotating wheels. J Dyn Syst Meas Control 2003;125(3):354–60.
[9] Braghin F, Bruni S, Resta F. Active yaw damper for the improvement of railway vehicle stability and curving performances: simulations and experimental results. Veh Syst Dyn 2006;44(11):857–69.
[10] Shen G, Goodall R. Active yaw relaxation for improved bogie performance. Veh Syst Dyn 1997;28(4–5):273–89.
[11] Ward CP, Goodall RM, Dixon R, Charles GA. Adhesion estimation at the wheel-rail interface using advanced model-based filtering. Veh Syst Dyn 2012;50(12):1797–816.
[12] Pearson JT, Goodall RM, Mei TX, Himmelstein G. Active stability control strategies for a high speed bogie. Control Eng Pract 2004;12(11):1381–91.
[13] Wickens AH. The bogie vehicle. Fundamentals of rail vehicle dynamics, guidance and stability. Swets & Zeitlinger, Lisse, Netherlands; 2003. p. 174.
[14] Pérez J, Busturia JM, Mei TX, Vinolas J. Combined active steering and traction for mechatronic bogie vehicles with independently rotating wheels. Annu Rev Control 2004;28(2):207–17.
[15] SET L. Wheelmotor project. 2013. http://www.set.gb.com/innovation.php [accessed 23-May-2016].
[16] Julian S, Cooney N, Goodall RM, Sellick R. The use of wheelmotors to provide active steering and guidance for a light rail vehicle. The Stephenson conference: research for railways. 2017.
[17] RailEngineer. Track inspection at 125 mph. 2012. https://www.railengineer.uk/2012/11/28/track-inspection-at-125mph/ [accessed 19-January-2018];.
[18] Polach O, Berg M, Iwnicki S. Simulation. Handbook of railway vehicle dynamics. Taylor & Francis; 2006. p. 360–404.
[19] Perez J, Mauer L, Busturia JM. Design of active steering systems for bogie-Based railway vehicles with independently rotating wheels. Veh Syst Dyn 2002;37(sup1):209–20.
[20] Iwnicki S. Manchester benchmarks for rail vehicle simulation. Veh Syst Dyn 1998;30(3):295–313.
[21] Kalker JJ. Wheel-rail rolling contact theory. Wear 1991;144:243–61.
[22] Spiryagin M, Polach O, Cole C. Creep force modelling for rail traction vehicles based on the fastsim algorithm. Veh Syst Dyn 2013;51(11):1765–83.
[23] Goodall RM, Ward CP. Active control of railway bogies assessment of control strategies. Proceedings of the international symposium on speed-up and sustainable technology for railway and Maglev systems. Chiba, Japan; 2015.
[24] Dorf RC, Bishop RH. Modern control systems. 11th ed. Pearson9780132270281; 2008.
[25] RSSB. Track system requirements. 2007. https://www.rssb.co.uk/rgs/standards/GCRT5021%20Iss%203.pdf.

[26] Burstow M. VTAC calculator: guidance notes for determining $T\gamma$ values. Network Rail; 2012. http://www.networkrail.co.uk/cp5-access-charges/guide-to-determining-tgamma-values–vtac-calculator.pdf.
[27] MTS. Series 244 hydraulic actuators. https://www.mts.com/cs/groups/public/documents/library/dev_002093.pdf.
[28] Moog. A085 series hydraulic servo actuators. http://www.moog.com/products/actuators-servoactuators/industrial/hydraulic/a085-series-hydraulic-servo-actuators.html.
[29] Alstom. Motor catalogue. http://www.alstom.com/Global/Transport/Resources/Documents/brochure2014/Alstom%20Motors%20Catalogue%202015%20-%20English.pdf?epslanguage=en-GB.